Journal of Applied Organometallic Chemistry

2024, Volume 4, Issue 1

Original Article

Optimizing Mechanical Properties in Ternary Al-Si-Cu Alloys: Influence of Composition on Microstructure and Hardness

Fatima-Zahra Hachimi[a,*] | Yassine Hassani[a] | Bennaceur Ouaki[b] | Mohammed Ebn Touhami[a]

[a]*Laboratory of Advanced Materials and Engineering Process, Faculty of Science, University, Ibn Tofail, BP 133, 14000 Kenitra, Morocco*
[b]*Materials Engineer, National Higher School of Mines, Rabat, Morocco*

Use your device to scan and read the article online

Citation F.Z. Hachimi, Y. Hassani, B. Ouaki, M.E. Touhami, **Optimizing Mechanical Properties in Ternary Al-Si-Cu Alloys: Influence of Composition on Microstructure and Hardness.** *J. Appl. Organomet. Chem.*, **2024**, *4*(1), 62-75.

https://doi.org/10.48309/JAOC.2024.433221.1158

Article info:
Received: 6 January 2024
Accepted: 9 February 2024
Available Online: 21 February 2024
ID: JAOC-2401-1158
Checked for Plagiarism: Yes
Checked by Language Editor: Yes

Keywords:
Al-Si-Cu alloys, Casting, Growth, Hardness, Microstructure, Precipitation, Solidification

ABSTRACT

This study focused on optimizing the mechanical properties of ternary Al-Si-Cu alloys. Alloys near the eutectic composition (AS_5U_5, AS_5U_{10}, AS_5U_{15}, $AS_{10}U_5$, $AS_{10}U_{10}$, $AS_{10}U_{15}$, $AS_{15}U_5$, $AS_{15}U_{10}$, and $AS_{15}U_{15}$) were examined by melting and casting commercially pure metals (99.9% Al, 99.7% Si, and 99.9% Cu). Thermos-Calc software was used to analyze the precipitation phases and solidification process around the eutectic composition. Microstructural analysis, quantification of phases during solidification, and characterization using Scanning Electron Microscopy (SEM) with energy-dispersive X-ray analysis (EDX) were performed. Results revealed that the formation of the Al_2Cu component was unaffected by silicon content, but as copper content increased, the percentage of precipitated Al_2Cu increased, impacting the hardness of the alloys, especially at lower solidification temperatures.

Introduction

Aluminum constitutes 8% of the Earth's crust and its versatility positions it as the second most extensively utilized metal globally, following steel [1-3]. Common applications for aluminum include the production of foil and conductor cables [2].

To attain specific physical and mechanical properties, alloying aluminum with other elements and establishing the solidification conditions to enhance the strength required for diverse applications is necessary. For instance, when dealing with Kerman pliable clay, it is imperative to obtain samples in their pure form [4]. Consequently, aluminum serves various purposes across industrial sectors, including food preparation, energy generation, packaging, architecture, electrical transmission lines, and transportation. Depending on the specific application, aluminum exhibits versatility in

**Corresponding Authors: Fatima-zahra Hachimi* (fatimazahra.hachimi@uit.ac.ma)

substituting other materials such as copper, steel, zinc, tin plate, stainless steel, and titanium, among others. Casting is a method involving the melting of metals and their subsequent pouring into a mold to attain a desired solid shape. It stands out as the simplest, most cost-effective process and, at times, the sole technically viable means to achieve the required form. This approach is versatile, extending its applicability to a range of materials including metals, ceramics, plastics, and glass.

Among metals, aluminum alloys are extensively utilized in the automotive industry, primarily due to their favorable casting characteristics and mechanical properties. This can be largely attributed to the significant influence of silicon and copper, which enhance casting characteristics, as well as other physical attributes such as mechanical strength and corrosion resistance [5,6]. In addition, scanning electron microscope tests with X-ray dispersion can be conducted to identify the phases deposited after solidification [7,8]. Aluminum casting alloys, notably those containing silicon and copper, are widely utilized in various applications. Solidification is a process employed in diverse fields, including medicine, as seen in the solidification method of organic droplets. This method has been developed and validated using high-performance liquid chromatography with UV detection in human serum [9]. The amounts of both additions vary widely so that copper predominates in some alloys and silicon in others. In this present study, specific focus was given to the evolution of deposited phases during the solidification of aluminum alloys with additions of copper and silicon around the eutectic points [10]. The manufacturing of new aluminum-based alloys with different percentages of silicon and copper is also environmentally beneficial [11].

Concerning the addition of the copper element in aluminum alloys, it is evident that copper contributes to both strengthening and machinability, while silicon enhances castability and diminishes hot shortness. Alloys characterized by higher hypoeutectic silicon concentrations are typically more suitable for intricate castings and processes involving permanent mold and die-casting [12]. Certainly, the precipitation of the intermetallic compound Al_2Cu plays a pivotal role. Consequently, the incorporation of copper significantly augments both strength and hardness in both as-cast and heat-treated conditions [13]. Alloys featuring a copper content of 4 to 6% exhibit responsive behavior to thermal treatment, showcasing notably improved casting properties [14]. Furthermore, half or more of the copper is identified in the form of intermetallic compounds, predominantly $CuAl_2$ and Cu_2FeAl_7, as revealed by metallography. Metallography, in the broader sense, is the study of the internal structure of metals and alloys and its correlation with composition [15,16]. Regarding the silicon effect, aluminum-silicon alloys are typically more resistant to solidification cracking and display excellent castability and feeding characteristics [14, 17]. Alloys within the aluminum-silicon-copper family exhibit heat-treatable characteristics when the copper content is below 5.6% [1]. However, the alloys particularly significant in this category are those that additionally incorporate magnesium. This inclusion enhances the heat-treatment response, resulting in a desirable array of properties, notably premium strength capabilities.

The automotive and aerospace industries widely employ Al-Si-Cu alloys due to their outstanding castability, corrosion resistance, high specific strength, weldability, and low thermal expansion [18,19]. Several hypereutectic silicon alloys, containing silicon levels ranging from 12 to 30%, often include copper as well. The dominant silicon phase provides exceptional wear resistance, while the presence of copper contributes to matrix hardening and enhances strength at elevated temperatures [20].

Experimental

Manufacturing of samples and pre-treatment

To predict the formation of the probable phases and intermetallic compounds during the casting of aluminum-silicon-copper alloys with copper and silicon contents around the eutectic composition, numerical simulation using Thermo-Calc software 2021 was first used. Based on the results obtained by Thermo-Calc,

Table 1. Percentage of each element of the selected alloy

Sample	%Si	%Cu	%Al
AS5U5	5	5	90
AS5U10	5	10	85
AS5U15	5	15	80
AS10U5	10	5	85
AS10U10	10	10	80
AS10U15	10	15	75
AS15U5	15	5	80
AS15U10	15	10	75
AS15U15	15	15	70

samples were manufactured by melting commercially pure metals, i.e., 99.9% Al, 99.7% Si, and 99.9% Cu, in an electric furnace at 800 °C for 3 hours and mixed at every 30 minutes. After complete melting of the mixture and to approach the equilibrium conditions, the mixture was cast in a ceramic mold which is heated at 500 °C for a low cooling rate. The selected weight percent of aluminum, copper, and silicon of the manufactured samples are reported in Table 1.

Microstructure examination

Complete cooling of the samples is essential before commencing the metallographic preparation. This phase begins with the cutting of the samples, followed by meticulous cleaning using alcohol to remove any impurities. Subsequently, each set of three samples is secured using a Buehler coater.

Following this, the polishing process is initiated with a Buehler polisher. This stage commences with coarse polishing using a medium-sized abrasive paper (400-grit), followed by intermediate polishing with an (800-grit) paper to refine the surface. Finally, fine polishing is performed with a (1200-grit) paper to achieve a smooth surface.

To attain a shiny surface, an abrasive compound such as alumina oxide is applied to an abrasive cloth to complete the polishing process and achieve the desired surface quality. Finally, a chemical etching using hydrofluoric acid is carried out to prepare the sample for metallographic examination.

An example of samples prepared for metallographic examination is displayed in Figure 1.

The microstructures of all samples were examined using the Olympus optical microscope BX53MRF-S model, and the Perfect Image program V.8.0.0.9 analysis was used to determine the percentages of the deposited phases.

Scanning electron microscope (SEM) and EDX analysis

To characterize the nature of each deposited phase, we utilized the QUATTRO S-FEG scanning electron microscopy (SEM) provided by Thermo Fisher Scientific, in conjunction with energy-dispersive X-ray analysis (EDX).

Vickers hardness test

To understand the impact of copper and silicon content, the hardness values of the alloys were measured under casting conditions. This was done using the Vickers method with a 98 N load. It's noteworthy that the hardness samples used were the same as those utilized for microstructure analysis.

Figure 1. Example of coating sample

Results and Discussion

Microstructure and MEB-SEM analysis

Optical micrographs of the cast AS_5U_{10} and $AS_{15}U_{10}$ alloys are demonstrated in Figure 2 and Figure 3. As shown in the previous figures, the alloy has an α-Al dendritic matrix with dispersed needle-shaped eutectic silicon particles, as well as microstructural changes that occur with an increase in silicon content. Dark, contrasting intermetallic particles are visible in the images. Figure 4 and Figure 5 for the AS_5U_5 and AS_5U_{15} alloy show the use of backscattered electrons in SEM to identify these intermetallic phases. Cu containing intermetallic precipitates appears in white contrast and can be easily separated on SEM micrographs.

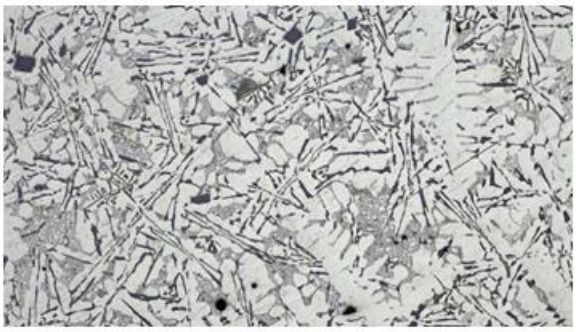

Figure 2. Microstructure of AS_5U_{10} alloy with x10 magnification taken by an optical microscope

Figure 3. Microstructure of the $AS_{15}U_{10}$ alloy with a magnification of x10 taken by an optical microscope

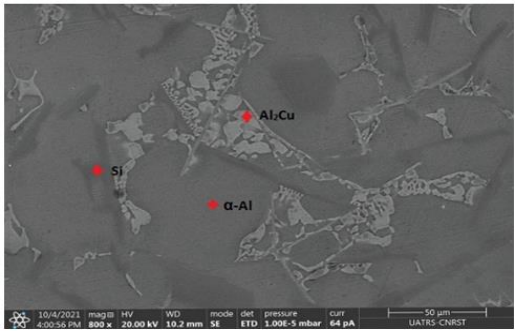

AS_5U_5

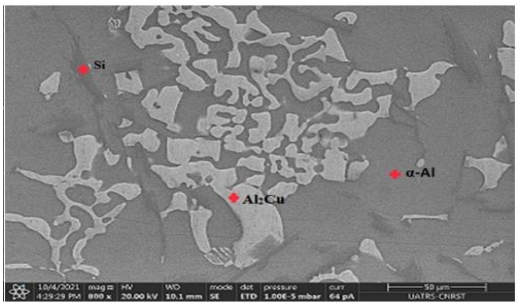

AS_5U_{15}

Figure 4. Example of microstructure analyzed by SEM of AS_5U_5 and AS_5U_{15} alloys

Base(2)

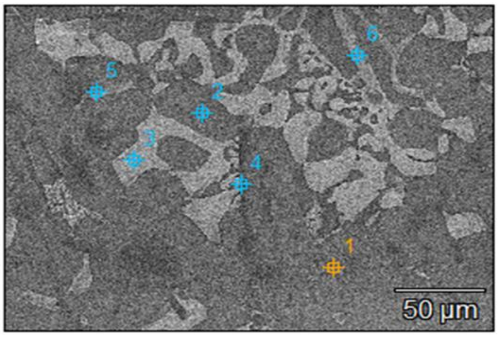

Figure 5. SEM micrograph of AS_5U_{15} alloy

Table 2. Chemical composition of the elements in each phase in point 1,3,4,5 of the AS_5U_{15} alloy

Elements	atomic %			
	Pt 1	Pt2	Pt3	Pt5
Al	69,66	63,36	9,74	61,97
Si	26,79	0,93	84,11	8,91
Cu	1,51	32,8	3,01	5,74
Cr	-	-	-	1
Mn	-	-	-	1,67
Fe	-	-	-	12,68

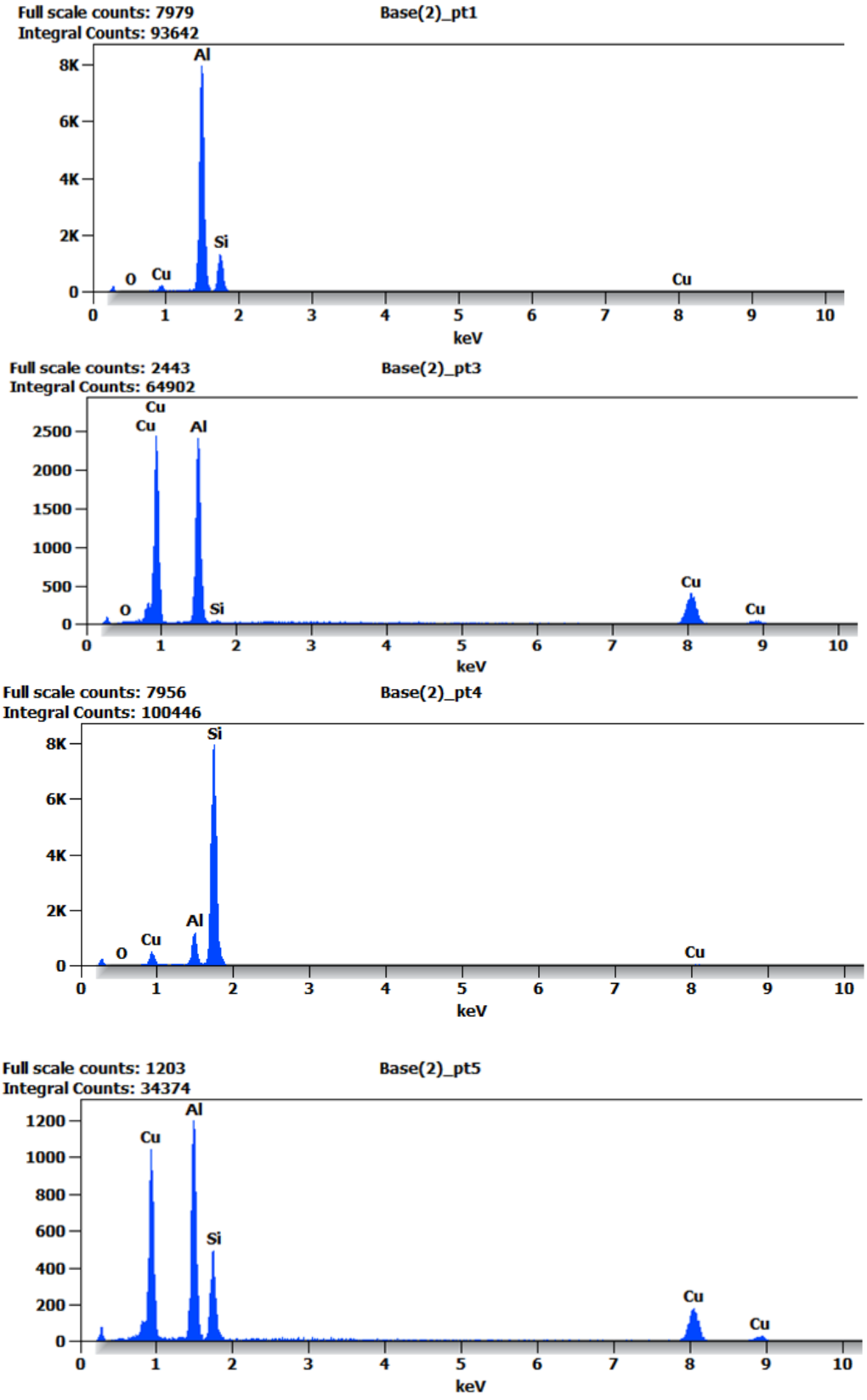

Figure 6. Spectrum of chemical analysis by EDX of the alloy AS_5U_{15} (points(1,3,4 et 5)

Table 2 presents the outcomes of spectra in Figure 6 of the EDX analysis conducted on the precipitate, denoted by the blue points in Figure 5. The EDX analysis confirms the presence of Cu in the sediment. The chemical composition of the intermetallic particle is identified as Al_2Cu, commonly referred to as the θ phase in Al-Cu alloys. The microstructure examined includes primary aluminum dendrites (light gray alpha phases), eutectic dendrites (mixture of alpha-matrix and dark gray spherical Si particles), and Cu- and Fe-rich intermetallic phases of various types, which are mainly concentrated in the spaces between the dendrites [21], as illustrated in Figure 3, Phases that incorporate copper and/or iron exhibit higher brightness in SEM secondary electron images due to elevated grayscale values. Eutectic is a mixture of Si particles and α matrices. The alpha matrix, comprising aluminum and silicon, initiates the precipitation of the liquid as the primary phase in the dendritic form- the anisotropic phase of silicon [21,22]. Intermetallic compounds include half or more of the copper [23]. Aluminum alloys exhibit intermetallic phases, like Al_2Cu, characterized by a tetragonal crystal structure. These phases undergo solidification, resulting in two distinct morphologies following the Al-Si eutectic reaction. The initial morphology appears in the form of large blocks (Al_2Cu, Figure 7a) with a notable copper concentration of approximately 38-40% Cu. In contrast, the second morphology manifests in a finely distributed ternary eutectic form (Al-Al_2Cu -Si, Figure 7 (b)). This variant is more common in the unaltered alloy and is identified either as distinct eutectic pockets or as precipitates on pre-existing silicon particles or iron phases [23-25]. Xing *et al.* studied the as-cast microstructure of foundry Al-Si-Cu alloy and Upon observation, it became evident that α-Al dendrites were encircled by eutectic Si phases and intermetallic compounds[26].

The eutectic Si phases manifested in lamellar and rod-like particles or as an Al-Si eutectic phase. The Cu-containing intermetallic compounds appeared in various morphologies-either as a eutectic phase, a block-like phase, or a combination of both, identified as Al_2Cu [8,19].

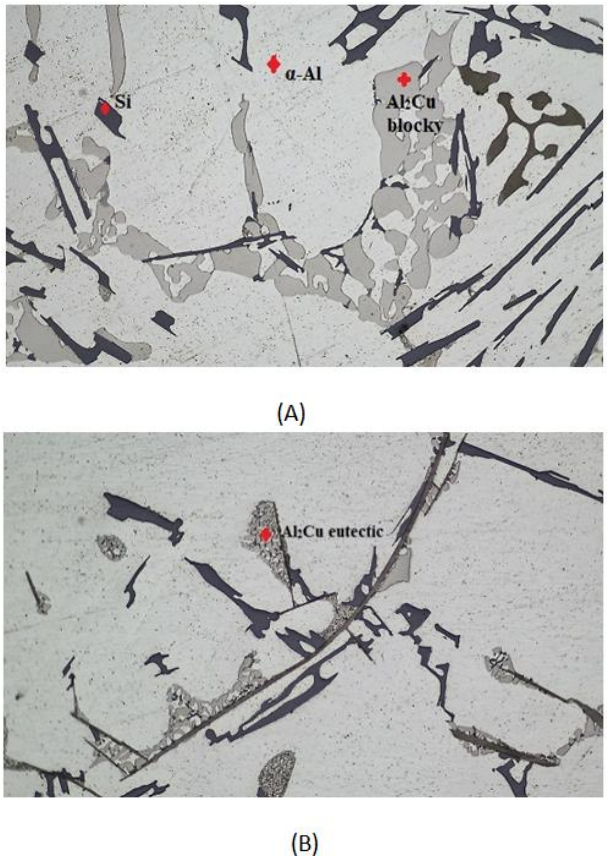

Figure 7. Microstructures of alloys (a) AS_5U_{10} and (b) $AS_{10}U_5$ at x50 magnification showing bulk Al_2Cu phases and ternary eutectic (Al- Al_2Cu -Si)

The experimental material was not refined or modified, so that the eutectic Si grows into platelets according to the double-plane reentrant edge mechanism (TPRE mechanism) along the preferred crystallographic directions. The Si wafers were most likely epitaxially grown from the surrounding primary aluminum dendrites. This result is in agreement with reports on Al-Si alloys which were not modified.

Theoretical aspect

The initiating influence of silicon, acting as a phase with crystallographic plates aligned with aluminum gates, exerts a substantial impact on the process of eutectic formation [22,23]. This is why silicon crystallization is the first step in the growth of a eutectic colony at 645.6 °C. Solid α-crystals from the solution form on the silicon crystals, which "wrap" the silicon pin and prevent its further growth in width due to the structural similarities [15,16]. The separation of

α(Al) microcrystals begins between a temperature of ≈ 615 °C and 540 °C in the tested alloys, and the precise temperature is primarily determined by the alloy's silicon and copper contents. The primary phase transforms into solid dendritic crystals, leading to elevated concentrations of copper and silicon in the residual liquid. The aluminium-silicon eutectic temperature, the first temperature plateau on the cooling curve, is between 570 and 555 °C, as shown in the cooling curves in Figure 8. The solid eutectic phase emerges within the gaps left between the dendritic arms, stabilizing at a constant temperature when the aluminum-silicon eutectic temperature is attained [27].
while the stable intermetallic phase Al_2Cu begins to precipitate at a constant temperature for all the alloys studied at a temperature of 521.6 °C, as summarized in Table 3.

Table 3. Percentage and the temperatures at the beginning and the end of the deposits of various obtained phases

	α-Al matrix		Si Crystal		Al_2Cu	
	Appearance temperature	Temperature of 25 °C	Appearance temperature	Temperature of 25 °C	Appearance temperature	Temperature of 25 °C
AS_5U_5	615.5	88.10%	556.7	5.96%	521.6	5.88%
AS_5U_{10}	599.4	81.61%	541.9	6.18%	521,6	12.20%
AS_5U_{15}	580.8	74.55%	531.2	6.42%	521,6	19.03%
$AS_{10}U_5$	579.7	82.34%	566.4	11.82%	521.6	5.83%
$AS_{10}U_{10}$	560.7	75.63%	556.9	12.26%	521.6	12.11%
$AS_{10}U_{15}$	564.1	68.4%	562.7	12.73%	521.6	18.86%
$AS_{15}U_5$	567.3	76.72%	623.2	17.58%	521.6	5.8%
$AS_{15}U_{10}$	556.3	69.75%	633.1	18.23%	521.6	12.0%
$AS_{15}U_{15}$	543.9	62.36%	645.9	19.00%	521.6	18.7%

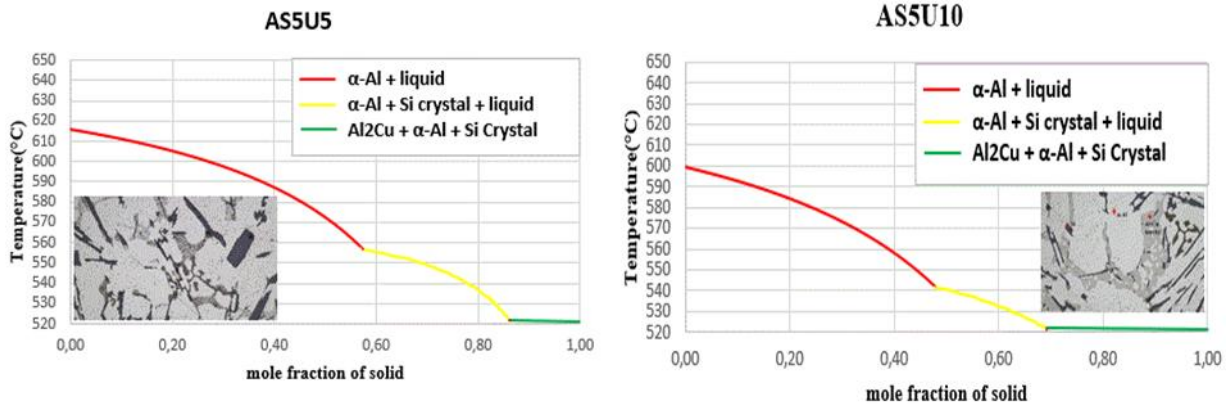

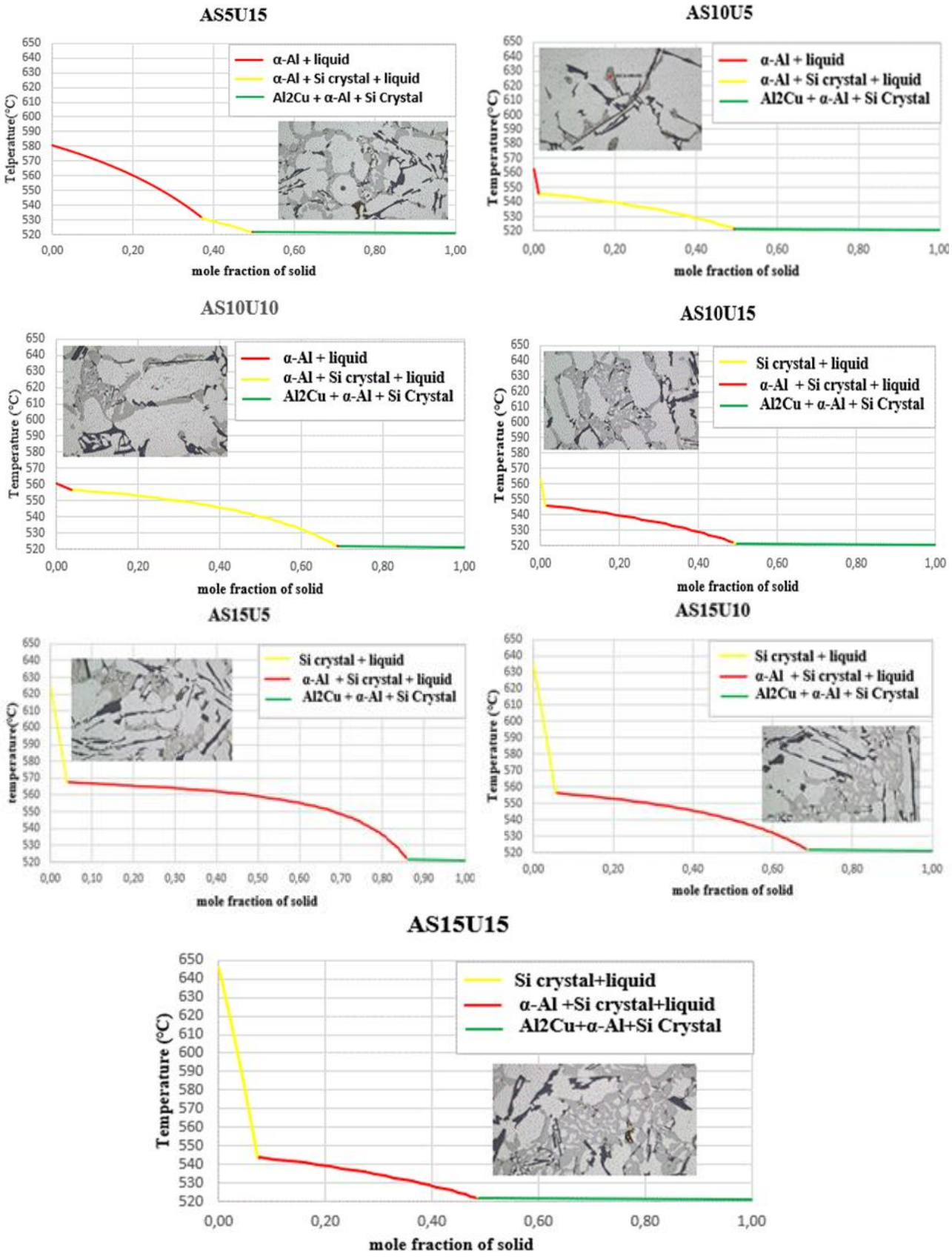

Figure 8. Solidification curves and microstructures

As crystals grow within a solid solution, silicon atoms align on the developing crystals and gather along the solid solution's crystallization front. This accumulation enriches adjacent casting layers with silicon, creating conditions conducive to the formation of silicon grains. Come back. The formation of silicon crystals in an α-solid solution is possible again after the surrounding casting becomes enriched with aluminium atoms. The sequential crystallization of silicon and a solid solution facilitates the development of eutectic colonies. Other silicon crystals are distributed on a silicon lamella at the same time Nevertheless, even with the concurrent deposition of the two eutectic phases, the moment two crystals of distinct phases merge at the boundary within the solid eutectic flow. One phase separate and another phase enriches the surrounding layer of the flow. This is why one phase is always in charge of crystallization and creates a framework, while the other is located in the intra-axis region of the framework. The significance of a phase is evaluated based on its linear rate of crystallization [22,23]. It was observed that at a temperature of 531 °C, the coarsening of primary Si particles concludes, and concurrently, the nucleation of the eutectic Al_2Si initiates. At this specific temperature, a portion of the residual molten alloy exhibited a eutectic composition, while certain precipitating Al2Si particles displayed a distinct eutectic appearance. The dendrite coherence point was observed at 568 °C. Therefore, after this temperature, the dendrites should not expand, but they continued to grow due to interdendritic feeding. The temperature at which the semi-solid slurry transitions to a rigid state, and the remaining liquid no longer flows freely, is referred to as the dendrite coherence point because the so-called skeleton begins to form and prevents free flow-movement of the residual molten metal [7]. Hence, it can be inferred that in all nine alloys, Al_2Cu was the final phase to undergo solidification, in conjunction with the low melting point elements. The microstructures depicted in Figure 2 and Figure 3 revealed the presence of intermetallic phases alongside primary silicon crystals and a solid solution (Al) once the solidification process concluded Their distribution, shape, and size depended on the cooling conditions.

Evolution des pourcentages des phases déposées et vitesse de solidification

Using Thermo-Calc simulation and quantitative analysis obtained by Perfect Image of samples, the evolution of the deposited phases was followed for different chosen compositions of the copper and silicon additions. Using perfect image analysis, a microstructure examination of samples was done. An example of the microstructure analyzed by perfect image is depicted in Figure 9.

The microstructure captured by the Perfect Image analysis software reveals three distinctive phases, distinguished by colors (blue, yellow, and red). According to the analyses conducted through EDX scanning electron microscopy in Figure 4, the red phase corresponds to the intermetallic compound Al_2Cu, the blue phase represents silicon crystals, and the yellow phase denotes the aluminum matrix. Focusing on the evolution of the percentage of Al_2Cu results obtained for each alloy by varying the mass proportions of copper and silicon are given in Table 4 and Figure 10. Examination of the results obtained shows that in each group which contains a fixed percentage of silicon and by varying the copper content, the percentage of formation of Al_2Cu increases as shown in Figure 10, which proves the positive influence of copper on aluminum silicon copper ternary alloys. However, the variation of the percentages of silicon does not reveal any importance on the Al_2Cu formation [28].

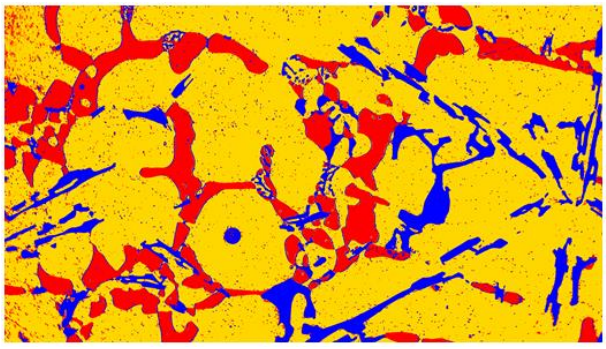

Figure 9. Example of a microstructure analyzed by perfect image software of AS_5U_{15} sample x50

Table 4. Percentages of Al_2Cu deposits results

	%Al_2Cu obtained by Thermo-Calc software	%Al_2Cu Obtained by Perfect Image analysis
AS_5U_5	5.88%	5.91%
AS_5U_{10}	12.20%	13.97%
AS_5U_{15}	19.03%	22.56%
$AS_{10}U_5$	5.83%	7.78%
$AS_{10}U_{10}$	12.11%	14.91%
$AS_{10}U_{15}$	18.86%	20.14%
$AS_{15}U_5$	5.80%	7.84%
$AS_{15}U_{10}$	12.00%	15.75%
$AS_{15}U_{15}$	18.70%	21.90%

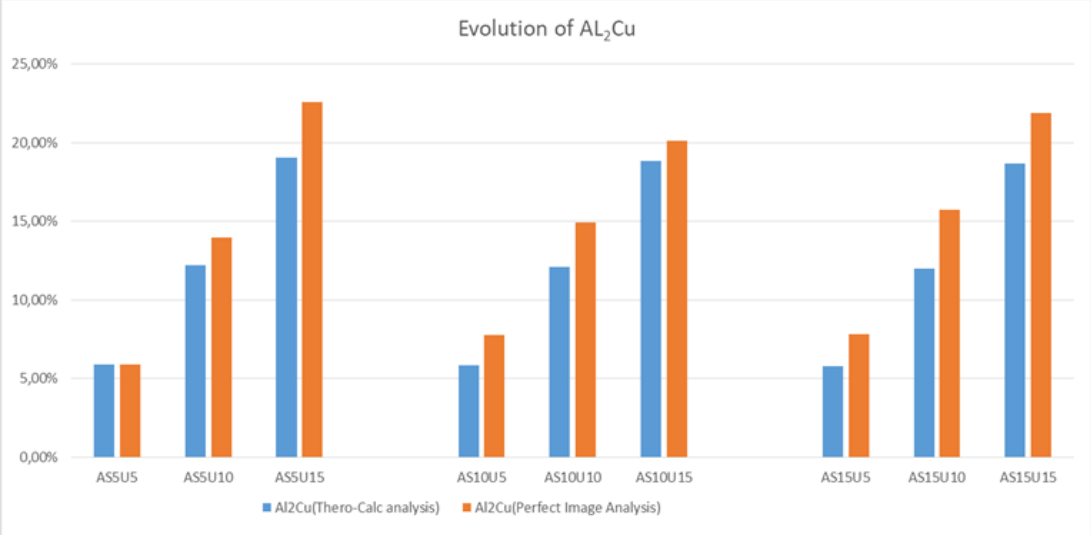

Figure 10. Evolution of Al_2Cu obtained by thermo-calc and perfect image analysis

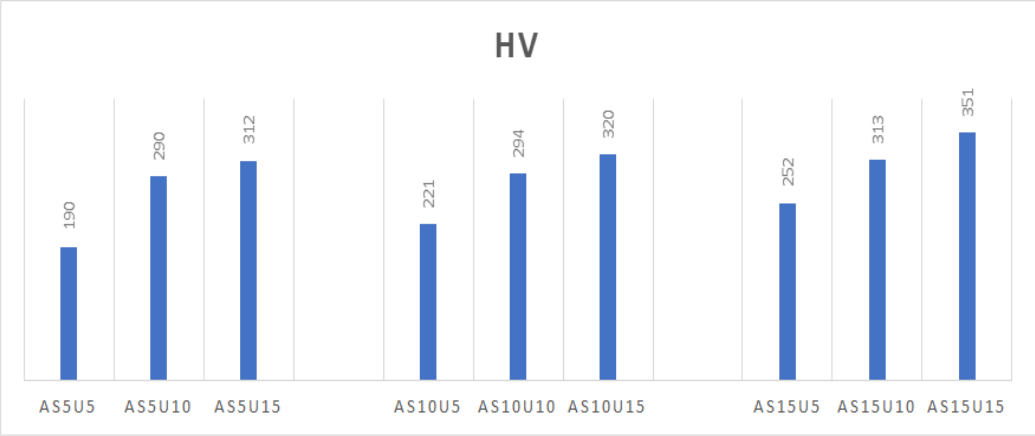

Figure 11. Hardness evolution of all the manufactured samples

Under the operating conditions chosen and by referring to the image analyses carried out on the various samples produced, it turns out that the influence of silicon on the formation of the compounds Al_2Cu is practically negligible [29]. Moreover, the comparison of the experimental data with the data obtained theoretically by thermo-Cal software shows only a small difference in the composition of Al_2Cu due to the presence of the impurities in the experiment.

Hardness evaluation

The mechanical properties of cast components are significantly influenced by the shape and distribution of silicon particles and intermetallic phases within the alpha (α) matrix. Due to the hardness but brittleness of Si platelets, which may crack and expose the soft α-matrix, this plate-like eutectic Si morphology is unfavorable for mechanical properties [30].

Thus, it is necessary to act on this morphology appropriately. Solution processing (under certain conditions) affects the morphological transformation kinetics of Si. The heat treatment process influences the size, shape, and distribution of precipitates in a cast component [31]. The evolution of hardness values of the alloys is graphed in Figure 11, we noted that all values given are an average of five measurements. By carrying out hardness measurements which allow us to have an idea of the evolution of the mechanical properties of such alloys around the eutectic composition, the measurement obtained shows a notable evolution of the hardness according to the percentage of copper for content silicon, as shown in Figure10. This increase, which is mainly attributed to the deposition of the Al_2Cu precipitate [32-35]. A thorough analysis of Figure 10 reveals that, while keeping the Cu content constant and adjusting the Si content, the hardness of the Al-Si-Cu alloy consistently rises. Therefore, the impact of silicon on hardness should not be overlooked, as it increases with varying percentages of the latter [36,37].

Conclusion

Based on Thermos-Calc software analysis of samples fabricated around the eutectic composition of Al-Cu-Si alloys, the phases deposited and their percentages could be predicted. The results showed that the effect of copper was significant, with an increase in its percentage leading to an increase in Al_2Cu deposition. The use of Perfect Image Analyzer and SEM-EDX confirms that the main deposited phases consist of Al- α Silicon crystals and Al_2Cu components. The intermetallic compound Al_2Cu is deposited in several morphologies (In various configurations, the precipitates can appear as a compact block-like Al_2Cu phase, a eutectic Al_2Cu phase, or a combination of both). Results confirm that the evolution of copper and Al_2Cu is simultaneous which influences the Al-Si-Cu alloys positively. On the other hand, the variation of silicon in the alloys proves to be of no importance in the formation of Al_2Cu. The rise in copper and silicon content correlates with an increased hardness, demonstrating the positive impact of both the intermetallic compound Al_2Cu and the presence of silicon on the mechanical behavior of the alloys. In this study, the fabrication of these new alloys has allowed us to discover that it is possible to create alloys with different percentages of components, thereby yielding results with good mechanical properties applicable in various fields. Enhancing this work with additional tests, such as corrosion testing, for instance, or through heat treatment, would be an interesting avenue to further explore.

Acknowledgements

We would like to express our deep gratitude to all individuals and institutions who have contributed, directly or indirectly, to the completion of this research. First and foremost, we sincerely thank Professor Mohamed Ebn Touhami and Professor Bennaceur Ouaki for their attentive supervision and insightful guidance throughout this project. We are also grateful to Hassani Yassine, who generously devoted his time to constructive discussions and insightful feedback, thereby enhancing the

quality of our work. Finally, we extend our appreciation to this supportive community that has made the accomplishment of this research possible.

Orcid

Fatima-Zahra Hachimi
https://orcid.org/0009-0005-8121-2500

Yassine Hassani
https://orcid.org/0009-0004-4196-5287

Bennaceur Ouaki
https://orcid.org/0000-0001-7999-8771

Mohammed Ebn Touhami
https://orcid.org/0009-0003-6383-8230

References

[1]. T. Alam, A.H. Ansari, Review on aluminium and its alloys for automotive applications, *International Journal of Advanced Technology In Engineering and Science*, **2017**, *5*, 278-294. [Google Scholar], [Publisher]

[2]. E.L. Rooy, Introduction to aluminum and aluminum alloys, **1990**. [Crossref], [Google Scholar], [Publisher]

[3]. M. Sajjadnejad, Y. Behnamian, Investigating the fracture properties of 316 stainless steel, *Advanced Journal of Chemistry, Section A*, **2024**, *7*, 190–208. [Crossref], [Publisher]

[4]. M. Dousti, A. Firoozfar, Different permeants and different additives, *Journal of Engineering in Industrial Research*, **2022**, *3*, 54–68. [Crossref], [Google Scholar], [Publisher]

[5]. M. Djurdjevič, M. Grzinčič, The effect of major alloying elements on the size of secondary dendrite arm spacing in the As-Cast Al-Si-Cu alloys, *Archives of Foundry engineering*, **2012**, *12*, 19–24. [Crossref], [Google Scholar], [Publisher]

[6]. P. Gómez, D. Elduque, J. Sarasa, C. Pina, C. Javierre, Influence of composition on the environmental impact of a cast aluminum alloy, *Materials*, **2016**, *9*, 412. [Crossref], [Google Scholar], [Publisher]

[7]. M. Sajjadnejad, S. Karkon, S.M.S. Haghshenas, Corrosion characteristics of Zn-TiO_2 nanocomposite coatings fabricated by electro-codeposition process, *Advanced Journal of Chemistry, Section A*, **2024**, *7*, 209–226. [Crossref], [Google Scholar], [Publisher]

[8]. S.E. Mousavi Ghahfarokhi, K. Helfi, M. Zargar Shoushtari, Synthesis of the single-phase bismuth ferrite ($BiFeO_3$) nanoparticle and investigation of their structural, magnetic, optical and photocatalytic properties, *Advanced Journal of Chemistry, Section A*, **2022**, *5*, 45–58. [Crossref], [Google Scholar], [Publisher]

[9]. A.H. Mohammad Shafiee, M.R. Mohammad Shafiee, Determination of clozapine by air assisted dispersive liquid-liquid microextraction based on solidification of organic droplet followed by HPLC in human serum, *Advanced Journal of Chemistry, Section A*, **2020**, *3*, 111–121. [Crossref], [Publisher]

[10]. A. Majumder, D. Chatterjee, S. Nandy, On the primary silicon precipitation during the eutectic solidification of Al–Si alloys, *Modelling and Simulation in Materials Science and Engineering*, **2023**, *31*, 075004. [Crossref], [Google Scholar], [Publisher]

[11]. S.J. Aghbolagh, Investigating standard environmental management in industries (Case study of oil industry), *Journal of Engineering in Industrial Research*, **2023**, *4*, 9–21. [Crossref], [Publisher]

[12]. L. Dobrzanski, R. Maniara, J. Sokolowski, The effect of cooling rate on microstructure and mechanical properties of AC AlSi9Cu alloy, *Archives of Materials Science*, **2007**, *106*, 106. [Google Scholar], [Publisher]

[13]. T. Gödecke, F. Sommer, Solidification behaviour of the Al_2Cu phase, *International Journal of Materials Research*, **1996**, *87*, 581-586. [Crossref], [Google Scholar], [Publisher]

[14]. M.H. Abdelaziz, A.M. Samuel, H.W. Doty, S. Valtierra, F.H. Samuel, Effect of additives on the microstructure and tensile properties of Al–Si

alloys, *Journal of Materials Research and Technology*, **2019**, *8*, 2255-2268. [Crossref], [Google Scholar], [Publisher]

[15]. D. Zhang, J. Peng, G. Huang, D. Zeng, Microstructure evolution of cast Al-Si-Cu alloys in solution treatment, *Journal of Wuhan University of Technology-Mater. Sci. Ed.*, **2008**, *23*, 184-188. [Crossref], [Google Scholar], [Publisher]

[16]. M. Karimi, Investigating the microscopic structure of cast Iron and its application in industry, *Journal of Engineering in Industrial Research*, **2023**, *4*, 77–85. [Crossref], [Publisher]

[17]. G.F. Vander Voort, J. Asensio-Lozano, The al-si phase diagram, *Microscopy and Microanalysis*, **2009**, *15*, 60-61. [Crossref], [Google Scholar], [Publisher]

[18]. I. Bacaicoa, M. Wicke, M. Luetje, F. Zeismann, A. Brueckner-Foit, A. Geisert, M. Fehlbier, Characterization of casting defects in a Fe-rich Al-Si-Cu alloy by microtomography and finite element analysis, *Engineering Fracture Mechanics*, **2017**, *183*, 159-169. [Crossref], [Google Scholar], [Publisher]

[19]. L.A.d.S. Baptista, A.F. Ferreira, K.G. Paradela, D.M.d. Silva, J.A.d. Castro, Experimental investigation of ternary Al-Si-Cu alloy solidified with unsteady-state heat flow conditions, *Materials Research*, **2018**, *21*. [Crossref], [Google Scholar], [Publisher]

[20]. O. Zobac, A. Kroupa, A. Zemanova, K.W. Richter, Experimental description of the Al-Cu binary phase diagram, *Metallurgical and Materials Transactions A*, **2019**, *50*, 3805-3815. [Crossref], [Google Scholar], [Publisher]

[21]. J.T. Kim, S.W. Lee, S.H. Hong, H.J. Park, J.Y. Park, N. Lee, Y. Seo, W.M. Wang, J.M. Park, K.B. Kim, Understanding the relationship between microstructure and mechanical properties of Al–Cu–Si ultrafine eutectic composites, *Materials & Design*, **2016**, *92*, 1038-1045. [Crossref], [Google Scholar], [Publisher]

[22]. L. Hurtalova, E. Tillova, M. Chalupova, The structure analysis of secondary (recycled) $AlSi_9Cu_3$ cast alloy with and without heat treatment, *Engineering Transactions*, **2013**, *61*, 197–218. [Google Scholar], [Publisher]

[23]. L. Dobrzański, W. Borek, R. Maniara, Influence of the crystallization condition on Al-Si-Cu casting alloys structure, *Journal of Achievements in Materials and Manufacturing Engineering*, **2006**, *18*, 211-214. [Google Scholar], [Publisher]

[24]. J. Yi, Y. Gao, P. Lee, T. Lindley, Effect of Fe-content on fatigue crack initiation and propagation in a cast aluminum–silicon alloy (A356–T6), *Materials Science and Engineering: A*, **2004**, *386*, 396-407. [Crossref], [Google Scholar], [Publisher]

[25]. L. Hurtalová, E. Tillová, M. Chalupová, Cu-rich intermetallic phases in recycled AlSi9Cu3 cast alloy–a comparison between aging behavior in T4 and T6 treatments, *Perners contacts–Electronical Technical Journal of Technology, Engineering and Logistic in Transport, VI*, **2011**, *2*, 72-80. [Crossref], [Google Scholar], [Publisher]

[26]. Y. Xing, Z. Jia, J. Li, L. Ding, H. Huang, Q. Liu, Microstructure and mechanical properties of foundry Al-Si-Cu-Hf alloy, *Materials Science and Engineering: A*, **2018**, *722*, 197-205. [Crossref], [Google Scholar], [Publisher]

[27]. M. Moustafa, F. Samuel, H. Doty, S. Valtierra, Effect of Mg and Cu additions on the microstructural characteristics and tensile properties of Sr-modified Al-Si eutectic alloys, *International Journal of Cast Metals Research*, **2002**, *14*, 235-253. [Crossref], [Google Scholar], [Publisher]

[28]. S. Jain, M. Patel, V. Kumar, S. Samal, Effect of Si on phase equilibria, mechanical properties and tribological behaviour of Al-Cu alloy, *Silicon*, **2023**, *15*, 1807-1820. [Crossref], [Google Scholar], [Publisher]

[29]. Y.A. Meyer, R.S. Bonatti, D. Costa, A.D. Bortolozo, W.R. Osorio, Compaction pressure and Si content effects on compressive strengths of Al/Si/Cu alloy composites, *Materials Science and Engineering: A*, **2020**, *770*, 138547. [Crossref], [Google Scholar], [Publisher]

[30]. V. Kumar, H. Mehdi, A. Kumar, Effect of silicon content on the mechanical properties of aluminum alloy, *International Research Journal of Engineering and Technology*, **2015**, *02*, 1326-1330. [Crossref], [Google Scholar], [Publisher]

[31]. J.M. Boileau, J.W. Zindel, J.E. Allison, The effect of solidification time on the mechanical properties in a cast A356-T6 aluminum alloy, *SAE transactions*, **1997**, 63-74. [Google Scholar], [Publisher]

[32]. E. Ashrafi, A. Hasan, H. Rashed, Effect of Cu in Al-Si alloys with phase modelling, *Industrial and Materials Engineering*, **2013**, *7*. [Crossref], [Google Scholar]

[33]. G. García-García, J. Espinoza-Cuadra, H. Mancha-Molinar, Copper content and cooling rate effects over second phase particles behavior in industrial aluminum–silicon alloy 319, *Materials & design*, **2007**, *28*, 428-433. [Crossref], [Google Scholar], [Publisher]

[34]. E. Sjölander, S. Seifeddine, The heat treatment of Al–Si–Cu–Mg casting alloys, *Journal of materials processing technology*, **2010**, *210*, 1249-1259. [Crossref], [Google Scholar], [Publisher]

[35]. R. Molina, P. Amalberto, M. Rosso, Mechanical characterization of aluminium alloys for high temperature applications Part1: Al-Si-Cu alloys, *Metallurgical Science and Tecnology*, **2011**, *29*. [Google Scholar], [Publisher]

[36]. H. Toda, T. Nishimura, K. Uesugi, Y. Suzuki, M. Kobayashi, Influence of high-temperature solution treatments on mechanical properties of an Al–Si–Cu aluminum alloy, *Acta Materialia*, **2010**, *58*, 2014-2025. [Crossref], [Google Scholar], [Publisher]

[37]. M. Zeren, Effect of copper and silicon content on mechanical properties in Al–Cu–Si–Mg alloys, *Journal of Materials Processing Technology*, **2005**, *169*, 292-298. [Crossref], [Google Scholar], [Publisher]